National Research FLAGSHIPS
Wealth from Oceans

CSIRO

IPCC AR4 climate model synthesis for the dynamical downscaling of the Leeuwin Current

Chaojiao Sun, Ming Feng, Richard Matear, and Matthew Chamberlain

9 June, 2009

[Insert ISBN or ISSN and Cataloguing-in-Publication (CIP) information here if required]

Contents

List of Figures

List of Tables

1. INTRODUCTION

The Leeuwin Current is the longest boundary current in the world oceans (Ridgway; Condie 2004). It carries warm, low-salinity tropical water poleward, affecting the coastal climate and ecosystems along the western and southern Australia (e.g., Waite et al. 2007). In a changing climate, how will it change and impact the regional climate and coastal ecosystems? In the recent IPCC Fourth Assessment Report (AR4), a warmer climate is predicted for the future by coupled climate models due to anthropogenic influences. However, these coarse-resolution climate models cannot resolve the Leeuwin current. To address this shortcoming, climate downscaling approaches have been adopted. In this project, a dynamical downscaling approach is being tested: an eddy-resolving ocean general circulation model, the BLUELink Ocean Forecasting Australia Model (OFAM), is used to simulate future ocean climate forced by large-scale climate model forcing. A statistical downscaling approach is currently under investigation.

However, before embarking on this journey, first we need to evaluate the accuracy of the climate model simulations. Since no validating observations exist for the future climate, the best we can do is to assess climate model simulations in terms of the current climate (Reichler; Kim 2008). Assuming that models capable of reproducing current climate are reliable in predicting future climate, a suitable climate model for climate downscaling of Leeuwin Current in the future climate can be identified, based on how well it simulates the present.

Studies have shown that the Indian Ocean has warmed up in the past 50 years (e.g., Alory and Meyers, 2009; Alory et al., 2007), the thermocline in the tropical Indian Ocean has shoaled (Cai et al., 2008), and the Leeuwin Current transport has weakened (Feng et al., 2008). How well can climate models simulate the current climate?

In this report, we evaluate several climate models which were identified by Reichler and Kim (2008) to be among the best performing models based on their simulations of the 20th century, with a focus on the factors which are most important for the Leeuwin Current. Reichler and Kim based their rankings of climate models on how well the climate models reproduce current time-mean climate signals. In this report, we focus on the simulation of wind stress and dynamic height by climate models, since these are good predictors of the Leeuwin Current. We evaluate both spatial and temporal variability of these variables simulated by the models. For future predictions, we focus on the A2 scenario from the IPCC AR4 report (denoted SRES A2), since it has tracked most closely the recent trend in the global temperature. We investigate climate model projections to gain insight into the likely evolution of the Leeuwin Current. In a companion technical report by Chamberlain et al. (2009), a test case of climate downscaling using the CSIRO climate model Mk3.5 is reported.

2. WIND STRESS SIMULATION FOR THE CLIMATE OF THE 20TH CENTURY AND ITS FUTURE TRENDS

Reichler and Kim (2008) evaluated three generations of IPCC climate models based on their comparison with the time mean of the current climate (Table 1). They developed a performance

index that is based on weighted difference of model simulation and all available observations (Fig. 1). Based on Reichler and Kim (2008), we focused on four climate models: GFDL-CM2.1, MPI-ECHAM5, UKMO-HadGEM1, and the CSIRO Mk3.5 climate model. The first three models are among the best performing climate models, and the last one was used in the test experiments of dynamical downscaling (Chamberlain et al., 2009). These four climate models have different resolutions in their ocean model component (Table 2), which affects their performance.

Since the Leeuwin Current is maintained by meridional pressure gradient established by the Indonesian Throughflow (e.g., Wijfles and Meyers 2004; Batteen et al. 2007), which is mainly driven by large-scale wind patterns in the Indian and Pacific Oceans (e.g., Feng et al. 2007, Domingues et al, 2007), we compare wind stress and wind stress curl patterns from IPCC AR4 climate model simulations with observations of the 20th century climate. We also compare the steric height simulated by climate models with CARS climatology.

We use atmospheric reanalyses as a proxy for observations of the current climate. ERA40 is a state-of-the-art atmospheric reanalysis product (Uppla et al., 2005) that incorporates satellite and in situ observations into an atmospheric general circulation model to provide the best estimate of the atmospheric state over a 45-year period (from 1957 to 2002). We use it as a benchmark to evaluate climate model performance, and loosely refer to it as the "observation". When appropriate, we also compare with other atmospheric reanalysis products, such as NCEP/NCAR Reanalysis (Kalnay et al., 1996; hereafter NCEP1) and NCEP/DOE AMIP II Reanalysis (Kanamitsu et al. 2002; Roads 2003; hereafter NCEP2), to establish confidence limits for the observations. NCEP1 is an atmospheric reanalysis products developed by NCEP. NCEP-2 is a rerun of NCEP-1 with the same input data and vertical and horizontal resolution, focusing on the period since 1979. NCEP2 improves the physical process and corrects some known errors in NCEP-1. Note that NCEP2 covers a shorter time period (1979 - present) as compared to NCEP1 (1948 - present).

2.1 Simulating present climate 1981-2000

Using ERA40 as a benchmark, we investigate bias in climate model simulation of the zonal wind stress. The difference between the time mean zonal wind stress from a climate model and ERA40 is computed over the tropical Pacific-Indian Oceans over a common 20-year time period (1981-2000). This difference represents the bias in the climate models. Overall, the GFDL coupled climate model CM2.1 has the smallest bias, while the other three models have significant bias south of 40ºS (Fig. 2).

As the Mk3.5 climate model is used in a downscaling test case, its performance in simulating present-day zonal wind stress in the Pacific and Indian Oceans is evaluated against several atmospheric reanalysis products, namely, the NCEP1, NCEP2 and ERA40 Reanalysis. In Fig. 3, zonally-averaged zonal wind stress (taux) averaged over two twenty-year periods (1951-1970 and 1981-2000) from Mk3.5 and the observations are shown. It is clear that there is a climate shift from the time period before the 1970s to the time period after 1970s, with an increase in the magnitude of the westerlies. This shift has been well documented in the literature, and attributed to contributions of anthropogenic forcing and decadal variability of the climate system (e.g., Trenberth and Hurrel 1994, Meehl et al., 2009, Cai et al. 2007). However, the

Mk3.5 climate model produces biased zonal wind in the Antarctica Circumpolar Current region, which is too large in both 20-year periods.

There is also an issue of using either monthly-averaged forcing fields or daily-averaged forcing fields to drive OFAM. The point of using daily-averaged fields is demonstrated in Fig. 4, which shows the comparison of standard deviation in daily vs. monthly zonal wind stress (taux) in ERA40 reanalysis averaged over 1981-2000. It is obvious that daily fields should be used by downscaling; otherwise the range of variability could be missed.

We also investigated simulated variability by Mk3.5 in the daily zonal wind as compared to that of the NCEP2 reanalysis (Fig. 5). The standard deviation of the zonal wind is computed over their common time period (1991-2000). There are substantial differences in the equatorial Pacific and Indian Oceans, as well as in the Southern Ocean.

Biases in the meridional wind stress in climate models are shown in Fig. 6. The Mk3.5 climate model has the largest bias in the Southern Ocean among the four climate models.

Sverdrup balance indicates that when there is a large change in the wind stress curl, a large change in the wind-driven ocean circulation can be expected (e.g., Cai et al., 2005). Using ERA40 as a proxy for the observations, we computed the modelled and observed (ERA40) wind stress curl (Fig. 7). The GFDL and UKMO climate models have smaller biases. However, the Mk3.5 has large positive and negative biases south of 30ºS, while the MPI climate model has very prominent negative biases south of 40ºS.

To see if there is significant different in wind stress curl by different atmospheric reanalysis products, the time mean of wind stress curl over 20 years (1980-1999) from NCEP2 and ERA40 are computed. Their difference is shown in Fig. 8. They are consistent over most of the southern oceans except in regions south of 60ºS.

2.2 Predicting future climate 2060-2080

It is also indicative to examine the trend in zonal wind stress to anticipate what kind of changes in the ocean circulation will likely occur in the Western Australian region. Figure 9 shows the trend simulated by the four climate models for years 2060-2080 for the A2 scenario (SRES A2). Interestingly, the GFDL climate model predicted the largest change in zonal wind stress in the Southern Ocean.

Figure 10 shows the trend in meridional wind stress. Mk3.5 predicts a large reduction of meridional wind stress in the Southern Pacific Ocean south of 40ºS, in disagreement with the other three climate model predictions.

The trend in wind stress curl for 2050-2100 is shown in Fig. 11. The GFDL and MPI coupled models are expected to project larger changes in the ocean circulation than the other two climate models due to a greater increase in wind stress curl.

3. STERIC HEIGHT SIMULATION IN THE LEEUWIN CURRENT REGION

The spatial resolution of climate models is too coarse to actually simulate the Leeuwin Current. However, it is well established that the Leeuwin Current is largely driven by a north-south pressure gradient (Godfrey; Ridgway 1985), which is quite broad zonally and meridionally. If this pressure gradient can be resolved by climate models, and if this pressure gradient can be used as a proxy of the strength of the Leeuwin Current, then we can make predictions of the Leeuwin Current in the future based on climate model projections. Here we examine how well the structure and patterns of this pressure gradient are simulated by various climate models, and compare with observations in the current climate. The simulations in the future climate are explored.

The time mean steric height (referenced to 300m) over a fifty-year period (1951-2000) of steric is calculated from the climate model simulations (Fig. 12). These are compared with steric height derived from observations: the CARS 2006 climatology (Ridgway et al. 2002; Dunn and Ridgway 2002). Overall, all climate models capture the patterns of the north-south gradient quite well. However, the CSIRO Mk3.5 climate model produced too strong a gradient. The coarse resolution of its ocean model (Table 2) is likely the cause. The UKMO model may not have enough vertical resolution to resolve the vertical structure to 300m depth. The two higher-resolution ocean models in GFDL-CM2.1 and MPI-ECHAM5 models seem to best capture the spatial pattern of steric height derived from CARS2006 climatology.

The fifty-year time mean of steric height over 2051-2100 is shown in Fig. 13. There are qualitative changes in the patterns, which are currently under further study for its implication on the Leeuwin Current in the future climate.

4. DISCUSSIONS AND EARLY FINDINGS

To make a reliable projection of future climate change on regional scales using dynamical downscaling, which requires a high-resolution ocean model, it is necessary to force the ocean model with the best available climate forcing. In this report, we have evaluated how well climate models simulate the current climate, as an indicator for future predictions. We focused on four climate models: three of them are among the best in simulating the time mean of the current climate; the fourth is the CSIRO climate model which is used in a test case for dynamical downscaling.

Overall, these climate models capture the variability and large scale patterns of the wind forcing, which is the main driver of the Leeuwin Current. The GFDL-CM2.1 climate model has the best performance with respect to simulating the wind stress and wind stress curl, as well as the steric height in the eastern Indian Ocean. Mk3.5 tends to have larger biases compared with other climate models.

In a test run, the CSIRO climate model Mk3.5 is used to dynamically downscale the OFAM (see the technical report by Chamberlain et al., 2009). The Mk3.5 is a coupled climate model developed by the CSIRO Marine and Atmospheric Research Division. The reason that Mk3.5 was used in the test run is that CSIRO scientists are familiar with this model and there exists a

climate run with the biogeochemical model coupled with it (Dietz et al., 2008). This test run will familiarize us with the climate downscaling methodology and serves as a learning tool. The rationale is that we will use what we learn from this downscaling experiment to make a climate projection using the best climate model once it is identified.

ACKNOWLEDGEMENT

We acknowledge the modeling groups, the Program for Climate Model Diagnosis and Intercomparison (PCMDI) and the WCRP's Working Group on Coupled Modelling (WGCM) for their roles in making available the WCRP CMIP3 multi-model dataset. Support of this dataset is provided by the Office of Science, U.S. Department of Energy. The ERA40 data is provided to CSIRO Marine and Atmospheric Research by the European Centre for Medium-Range Weather Forecasts. The NCEP/NCAR 1 and NCEP/DOE 2 Reanalysis data were provided by the NOAA/OAR/ESRL PSD, Boulder, Colorado, USA, from their Web site at http://www.cdc.noaa.gov/. We thank Peter Craig and Ken Ridgway for their valuable input. The final version benefited greatly from a thoughtful internal review by Graham Symonds. This work is supported by the WAMSI Node 2 project.

REFERENCES

Alory, G., and G. Meyers, 2009: Warming of the Upper Equatorial Indian Ocean and Changes in the Heat Budget (1960–99). *J. Climate*, **22**, 93–113.

Alory, G., S. Wijffels, and G. Meyers, 2007: Observed temperature trends in the Indian Ocean over 1960-1999 and associated mechanisms. *Geophysical Research Letters*, **34,** 6.

Batteen, M. L., R. A. Kennedy, and H. A. Miller, 2007: A process-oriented numerical study of currents, eddies and meanders in the Leeuwin Current System. *Deep-Sea Res. Part II-Top. Stud. Oceanogr.*, **54,** 859-883.

Cai, W., G. Shi, T. Cowan, D. Bi, and J. Ribbe, 2005: The response of the Southern Annular Mode, the East Australian Current, and the southern mid-latitude ocean circulation to global warming. *Geophysical Research Letters*, **32**.

Cai, W. J., and T. Cowan, 2007: Trends in Southern Hemisphere circulation in IPCC AR4 models over 1950-99: Ozone depletion versus greenhouse forcing. *Journal of Climate*, **20,** 681-693.

Cai, W., A. Sullivan, and T. Cowan, 2008: Shoaling of the off-equatorial south Indian Ocean thermocline: Is it driven by anthropogenic forcing? - art. no. L12711. *Geophysical Research Letters*, **35,** 12711-12711.

Chamberlain, M, R. Matear, M. Feng, and C. Sun, 2008: Dynamical downscaling of a climate change projection of ocean dynamics and biogeochemistry for the Australian region. In preparation.

Dietz, H., R. Matear, and T. Moore, 2008: The nitrogen budget in Anti-cyclonic eddies off western Australia based on eddy-resolving modeling and observations. Submitted.

Domingues, C. M., M. E. Maltrud, S. E. Wijffels, J. A. Church, and M. Tomczak, 2007: Simulated Lagrangian pathways between the Leeuwin Current System and the upper-ocean circulation of the southeast Indian Ocean. *Deep Sea Research Part II: Topical Studies in Oceanography*, **54,** 797-817.

Dunn J.R., and K.R. Ridgway, 2002: Mapping ocean properties in regions of complex topography, Deep Sea Research I : Oceanographic Research, 49 (3), 591-604.

Feng, M., S. Wijffels, S. Godfrey, and G. Meyers, 2005: Do eddies play a role in the momentum balance of the Leeuwin Current? *J. Phys. Oceanogr.*, **35,** 964-975.

Feng, M., L. J. Majewski, C. B. Fandry, and A. M. Waite, 2007: Characteristics of two counter-rotating eddies in the Leeuwin Current system off the Western Australian coast. *Deep Sea Research Part II: Topical Studies in Oceanography*, **54,** 961-980.

Feng, M., A. Biastoch, C. Böning, N. Caputi, and G. Meyers, 2008: Seasonal and interannual variations of upper ocean heat balance off the west coast of Australia, manuscript submitted.

Godfrey, J. S., and K. R. Ridgway, 1985: The Large-Scale Environment of the Poleward-Flowing Leeuwin Current, Western Australia: Longshore Steric Height Gradients, Wind Stresses and Geostrophic Flow. *J. Phys. Oceanogr.*, **15,** 481-495.

Kalnay, E., et al. (1996), The NCEP/NCAR 40-year reanalysis project, Bull. Am. Meteorol. Soc., 77(3), 437–471, doi:10.1175/1520-0477.

Kanamitsu, M., W. Ebisuzaki, J. Woollen, S.-K. Yang, J. J. Hnilo, M. Fiorino, and G. L. Potter (2002), NCEP-DOE AMIP-II reanalysis (R-2), Bull. Am. Meteorol. Soc., 83(11), 1631–1643, doi:10.1175/BAMS-83-11-1631.

Meehl, G. A., A. Hu, and B. D. Santer, 2009: The Mid-1970s Climate Shift in the Pacific and the Relative Roles of Forced versus Inherent Decadal Variability. *Journal of Climate*, **22,** 780-792.

Reichler, T., and J. Kim, 2008: How Well Do Coupled Models Simulate Today's Climate? *Bulletin of the American Meteorological Society*, **89,** 303-311.

Ridgway K.R., J.R. Dunn, and J.L. Wilkin, 2002: Ocean interpolation by four-dimensional least squares -Application to the waters around Australia, J. Atmos. Ocean. Tech., Vol 19, No 9, 1357-1375.

Ridgway, K. R., and S. A. Condie, 2004: The 5500-km-long boundary flow off western and southern Australia. *J. Geophys. Res.-Oceans*, **109,** 18.

Roads, J. (2003), The NCEP-NCAR, NCEP-DOE, and TRMM tropical atmosphere hydrologic cycles, J. Hydrometeorol., 4(5), 826–840, doi:10.1175/1525-7541.

Trenberth, K. E., and J. W. Hurrel (1994), Decadal atmosphere-ocean variations in the Pacific, Clim. Dyn., 9, 303–319.

Uppala, S.M., Kållberg, P.W., and coauthors, 2005: The ERA-40 re-analysis. Quart. J. R. Meteorol. Soc., 131, 2961-3012.doi:10.1256/qj.04.176

Waite, A. M., and Coauthors, 2007: The Leeuwin Current and its eddies: An introductory overview. *Deep-Sea Res. Part II-Top. Stud. Oceanogr.*, **54,** 789-796.

Wijffels, S., and G. Meyers (2004), An intersection of oceanic waveguides: Variability in the Indonesian Throughflow region, J. Phys. Oceanogr., 34, 1232–1253.

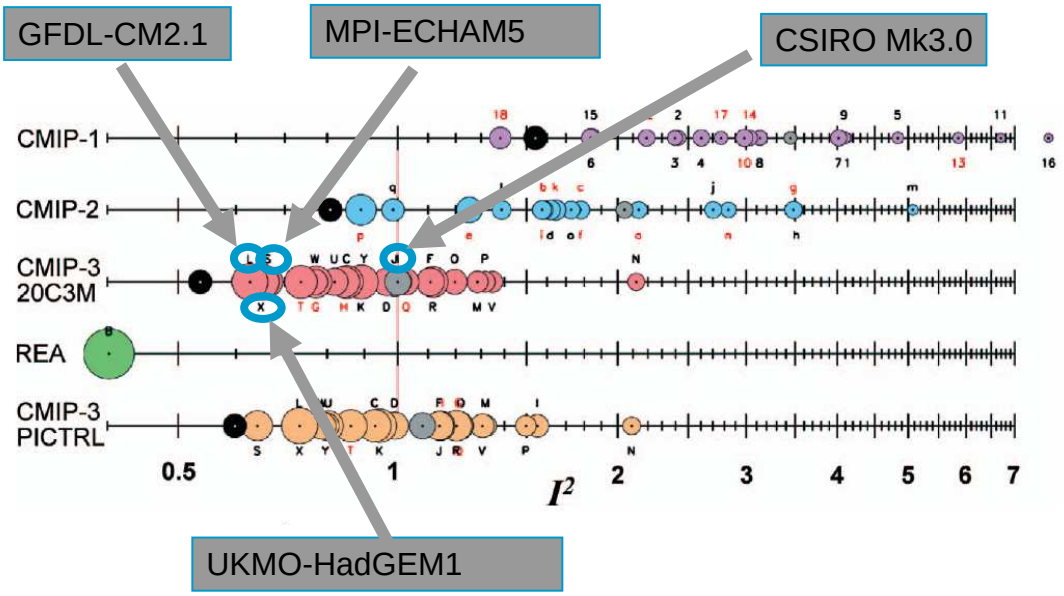

Figure 1: Performance index I^2 for individual models (circles) and model generations (rows). Best performing models have low I^2 values and are located toward the left. Circle sizes indicate the length of the 95% confidence intervals. Letters and numbers identify individual models (see supplemental online material at doi:10.1175/BAMS-89-3-Reichler); flux-corrected models are labeled in red. Grey circles show the average I^2 of all models within one model group. Black circles indicate the I^2 of the multimodel mean taken over one model group. The green circle (REA) corresponds to the I^2 of the NCEP/NCAR reanalyses. Last row (PICTRL) shows I^2 for the preindustrial control experiment of the CMIP-3 project. From (Reichler; Kim 2008) with permission.

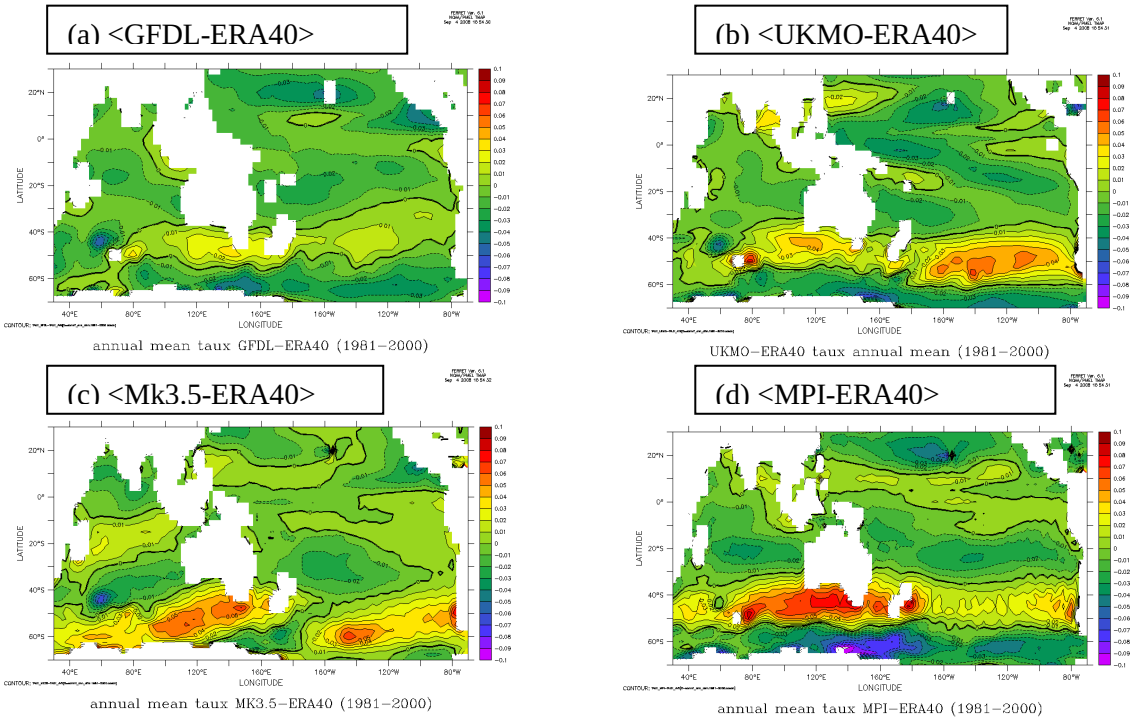

Figure 2: Zonal wind stress bias in climate models using the ERA40 reanalysis as a benchmark computed over 20 years (1981-2000). (a) Bias in GFDL climate model; (b) in UKMO; (c) in Mk3.5; and (d) in MPI.

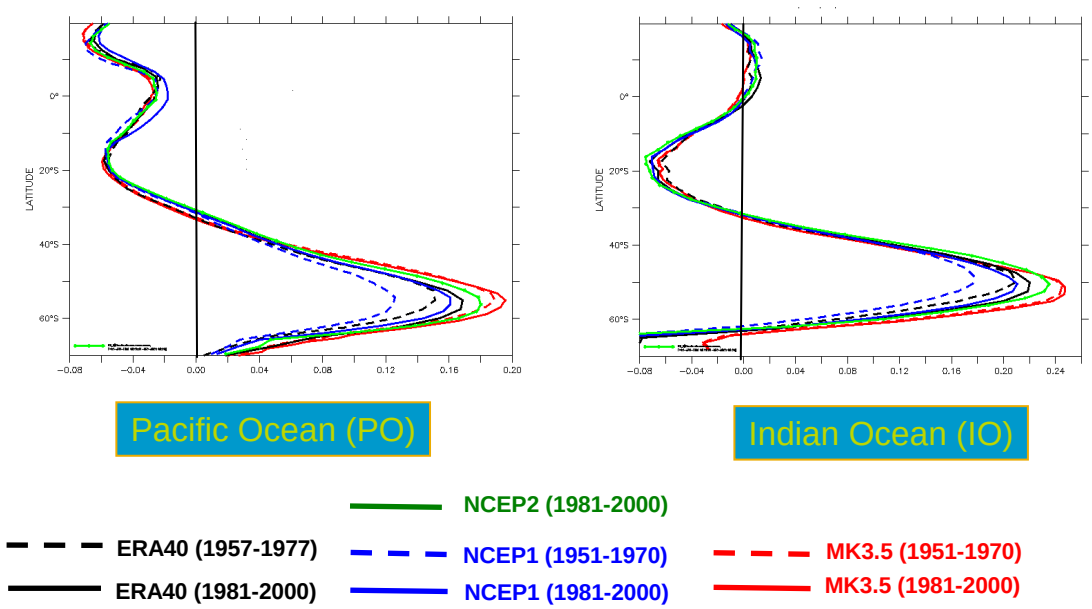

Figure 3: Zonally averaged taux (zonal wind stress) over two twenty-year periods: 1951-1970 and 1981-2000 for the Pacific Ocean basin (130E to 80W) and the Indian Ocean basin (30E to 130E).

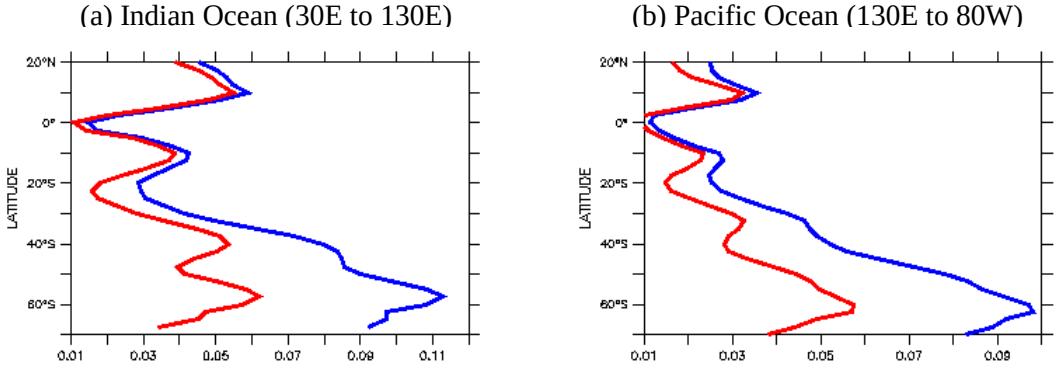

Figure 4: Standard deviation computed from daily (blue) and monthly (red) averaged ERA40 zonal wind field over 1981 to 2000.

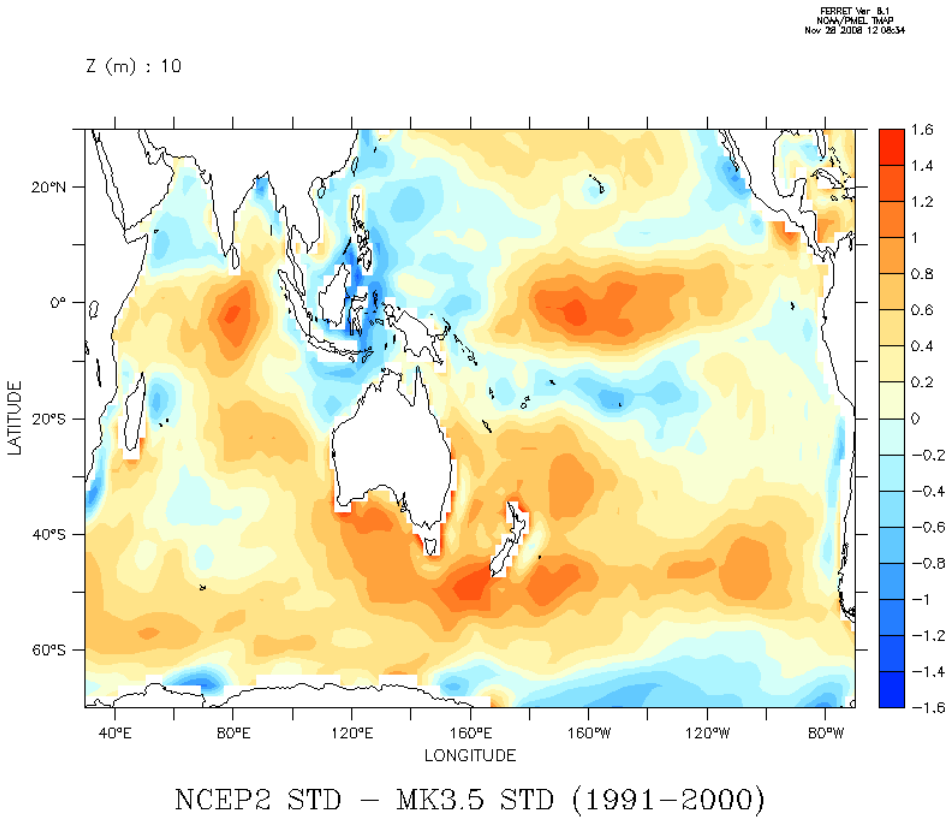

Figure 5: Difference in zonal wind standard deviation in NCEP2 and Mk3.5 (1991-2000).

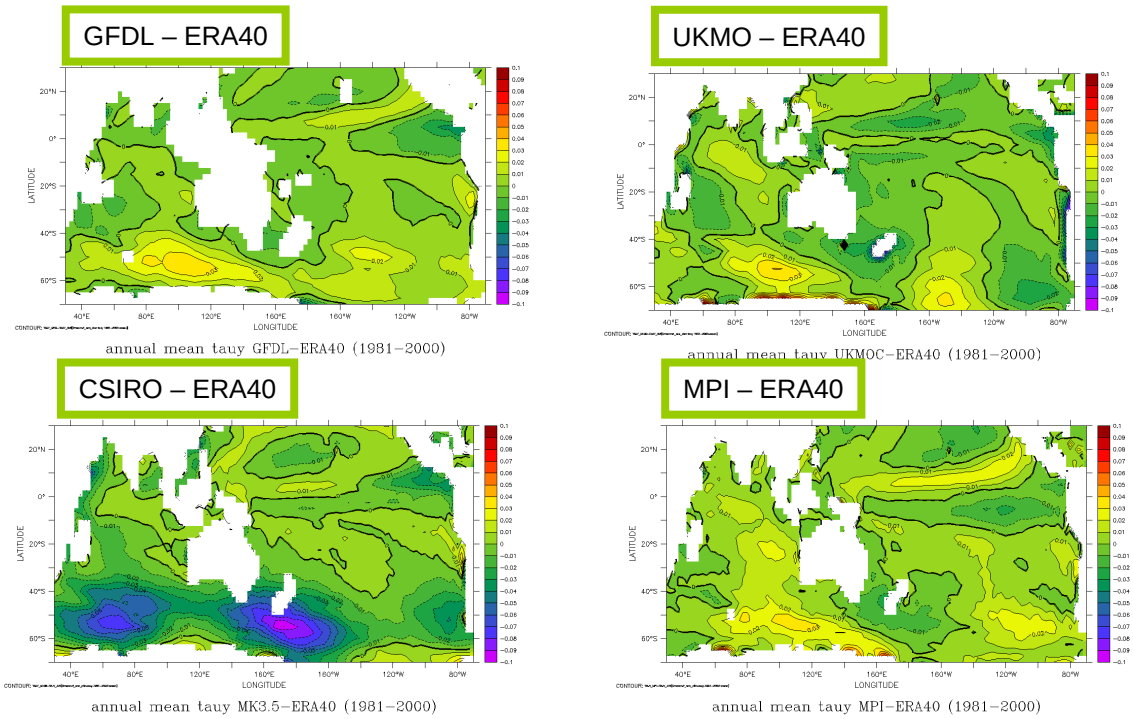

Figure 6: Same as in Fig.2, but for bias of meridional wind stress (tauy) in climate model simulations.

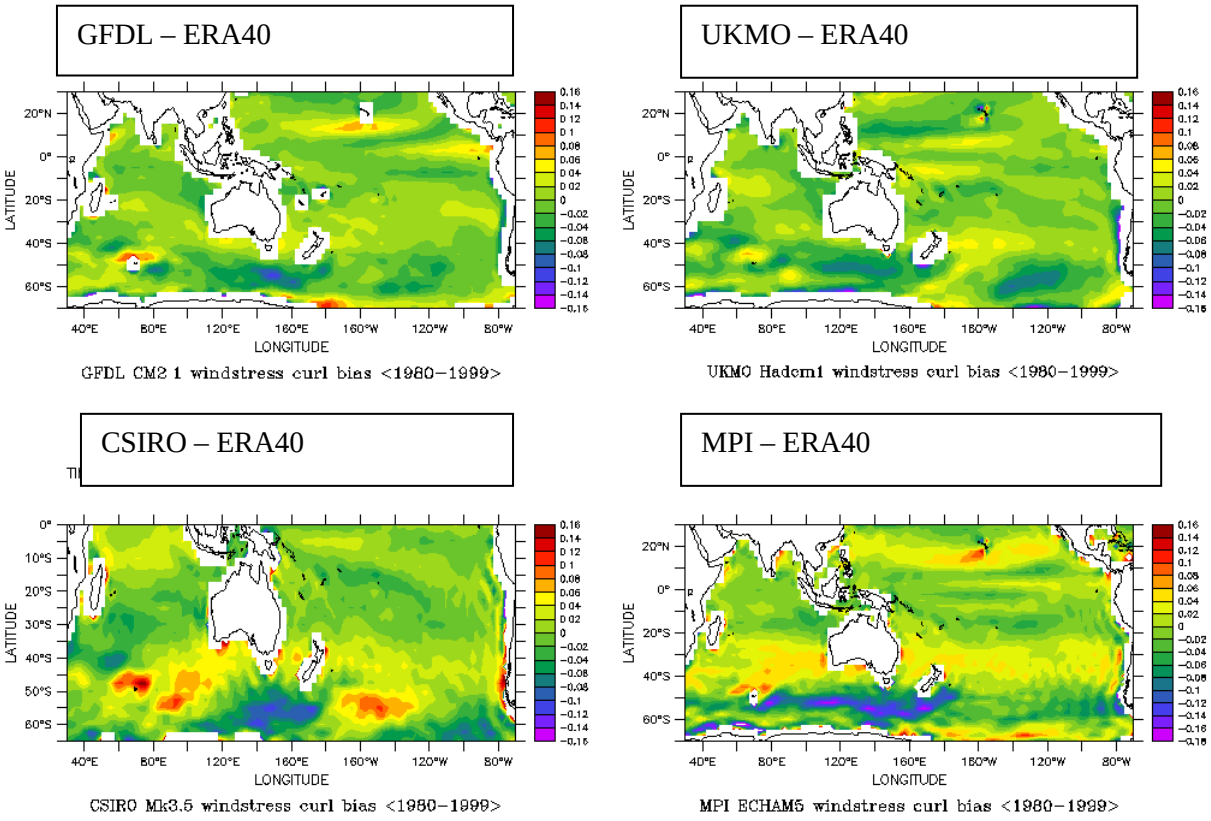

Figure 7: Biases in wind stress curl from climate models. ERA40 reanalysis data averaged over 1980-1999 is used as the benchmark.

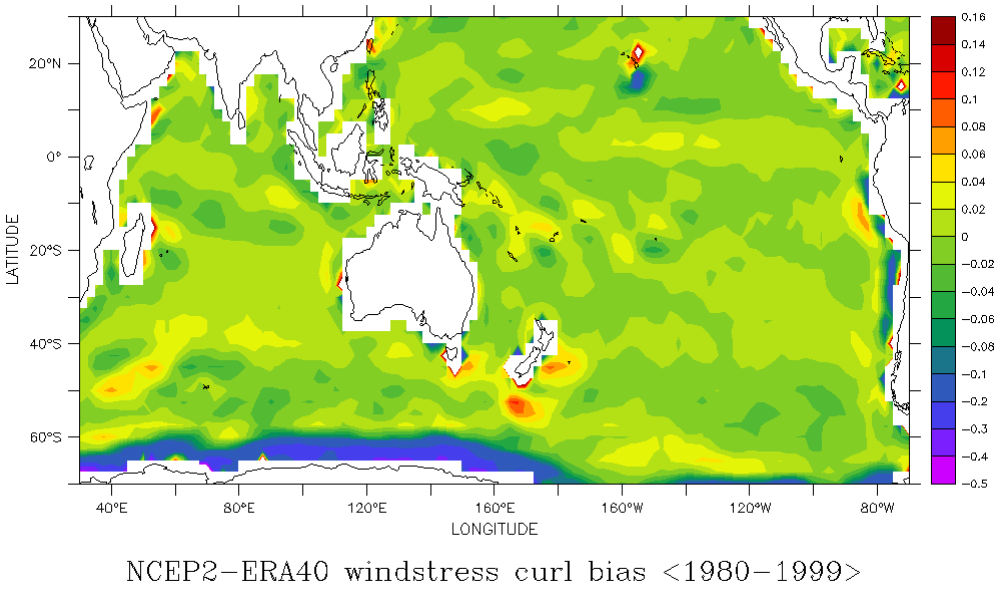

Figure 8: Difference in wind stress curl averaged over 20 years (1980-1999) from NCEP2 and ERA40 reanalyses.

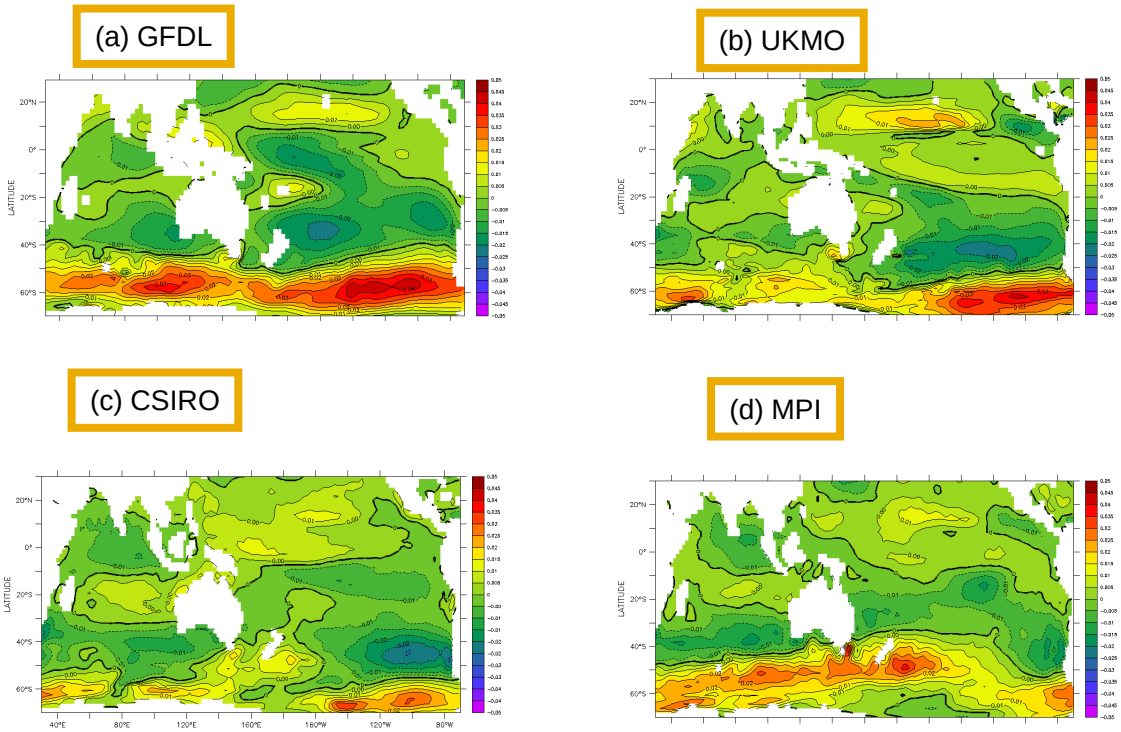

Figure 9: Trend in zonal wind stress from the climate models (SRES A2 – 20C3M). The trend is defined as the difference of two 20-year time periods: <2061-2080> - <1981-2000>.

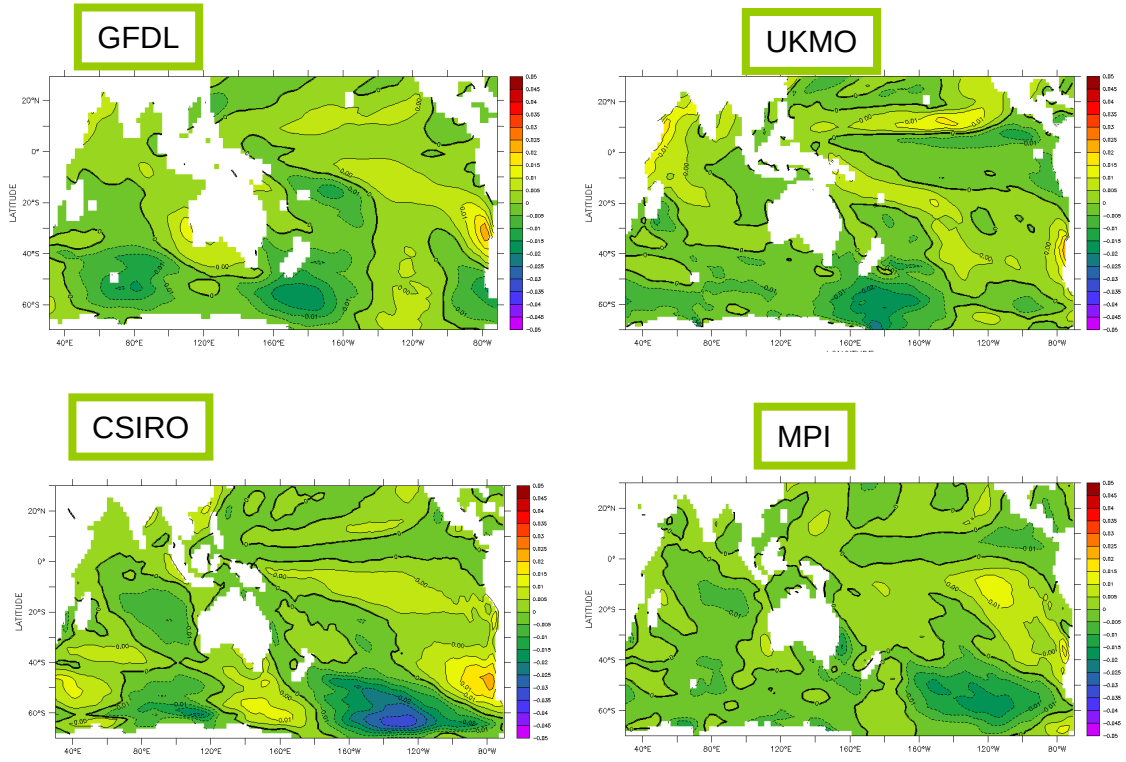

Figure 10: Trend in *meridional* wind stress τ^y from the climate models (SRES A2 – 20C3M). The trend is defined as the difference of two 20-year time periods: <2061-2080> - <1981-2000>.

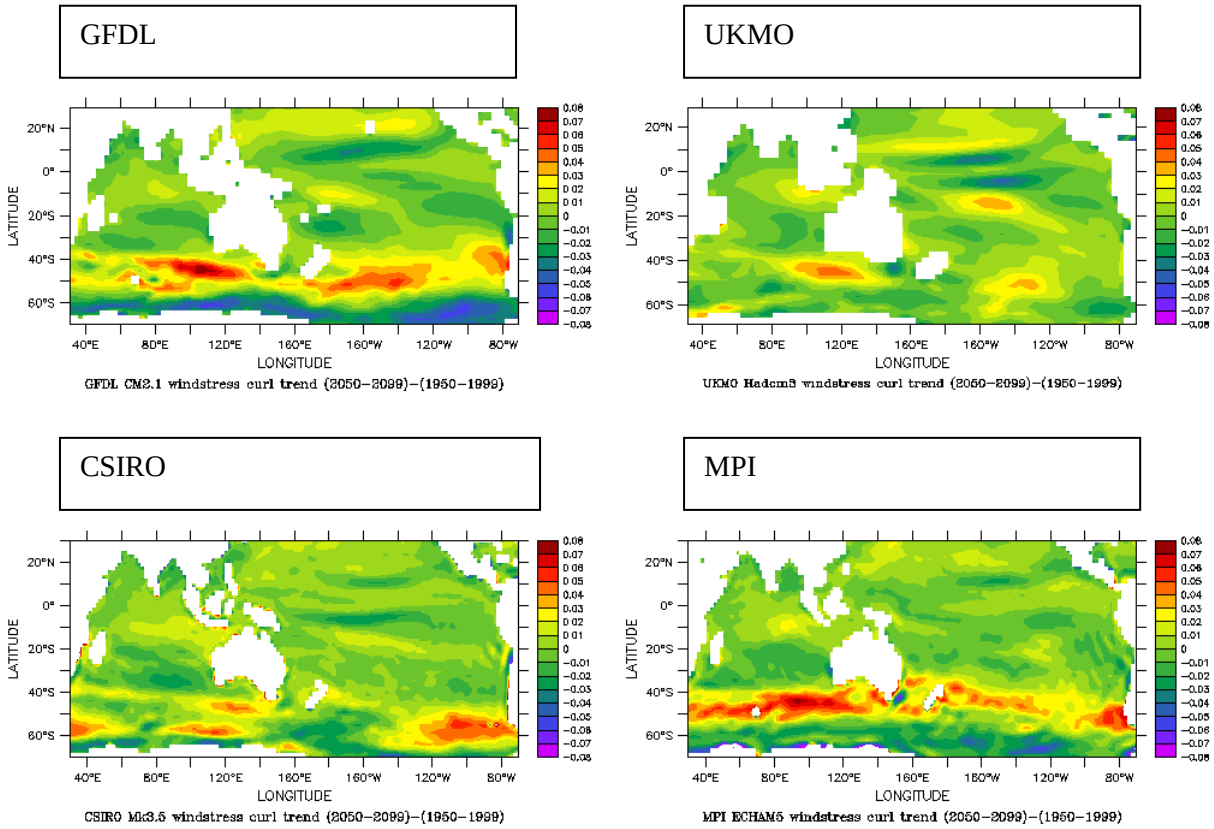

Figure 11: Trend in wind stress curl predicted from the climate models (SRES A2 – 20C3M). The trend is defined as the difference of two 50-year time periods: <2050-2099> - <1950-1999>.

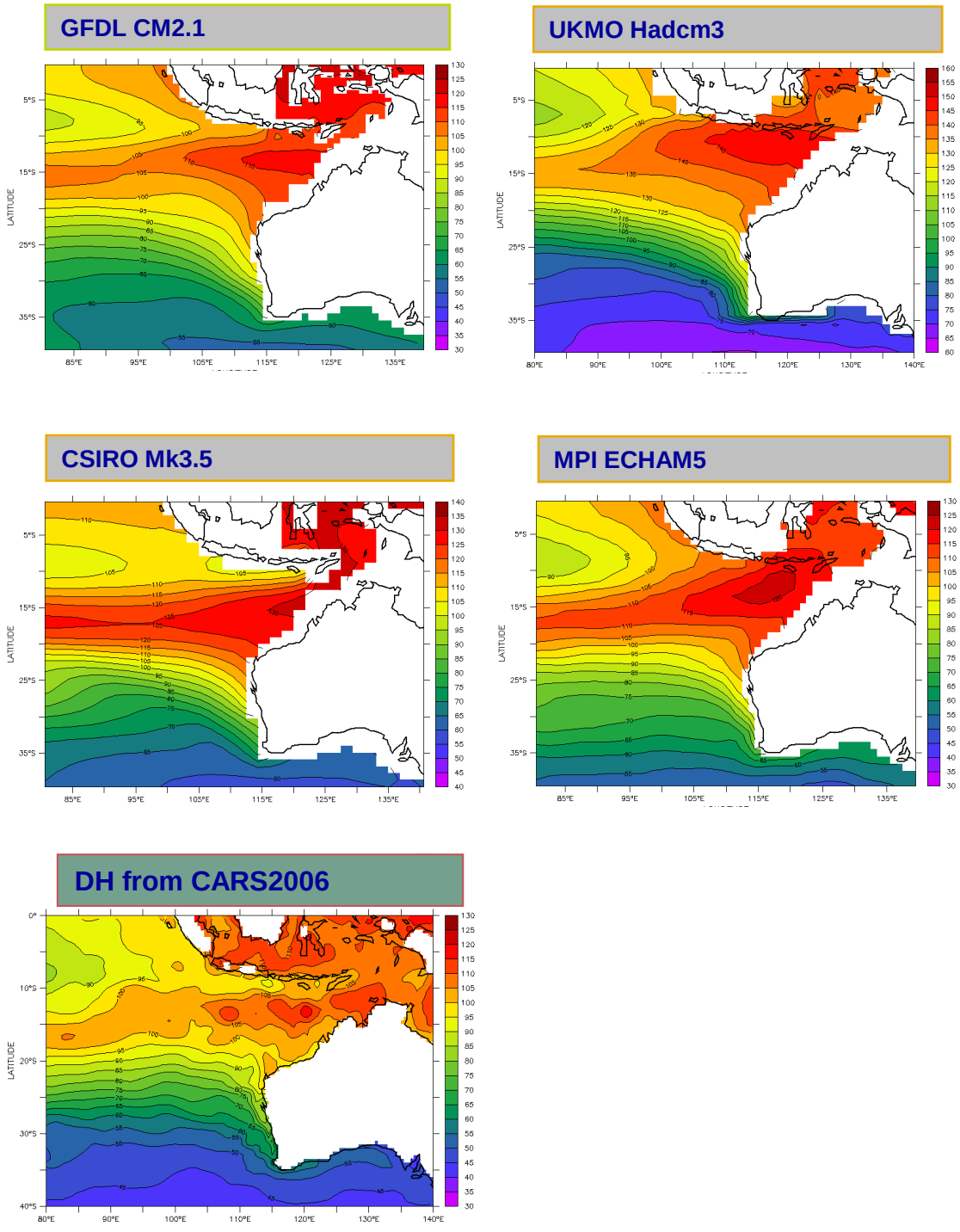

Figure 12: Dynamic height climatology from the four climate models over 1950-2000, and the climatology from observations in CARS2006.

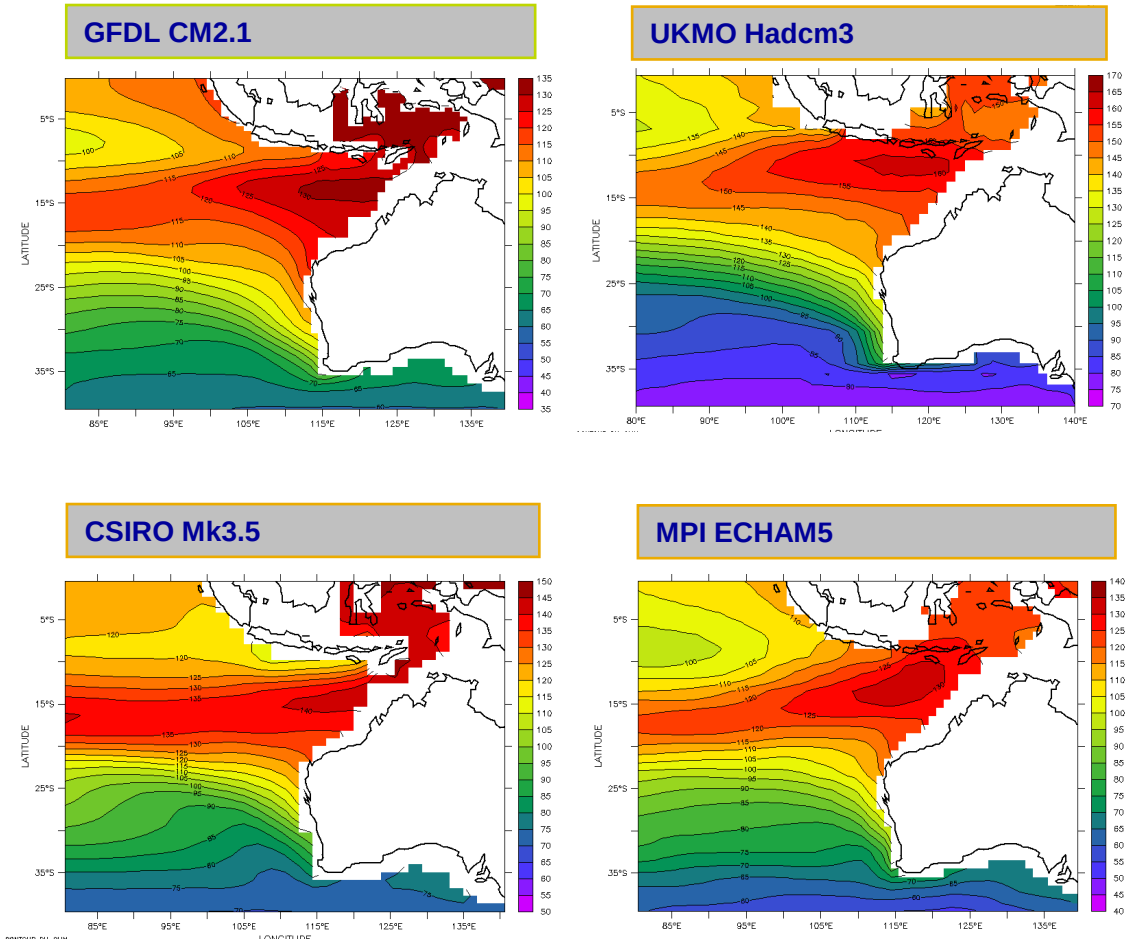

Figure 13: Dynamic height climatology in 2050-2100 for the four climate models.

Variable	Domain	Validation data	Period
Sea level pressure	ocean	ICOADS (Woodruff et al. 1987)	1979–99
Air temperature	zonal mean	ERA-40 (Simmons and Gibson 2000)	1979–99
Zonal wind stress	ocean	ICOADS (Woodruff et al. 1987)	1979–99
Meridional wind stress	ocean	ICOADS (Woodruff et al. 1987)	1979–99
2-m air temperature	global	CRU (Jones et al. 1999)	1979–99
Zonal wind	zonal mean	ERA-40 (Simmons and Gibson 2000)	1979–99
Meridional wind	zonal mean	ERA-40 (Simmons and Gibson 2000)	1979–99
Net surface heat flux	ocean	ISCCP (Zhang et al. 2004), OAFLUX (Yu et al. 2004)	1984 (1981) –99
Precipitation	global	CMAP (Xie and Arkin 1998)	1979–99
Specific humidity	zonal mean	ERA-40 (Simmons and Gibson 2000)	1979–99
Snow fraction	land	NSIDC (Armstrong et al. 2005)	1979–99
Sea surface temperature	ocean	GISST (Parker et al. 1995)	1979–99
Sea ice fraction	ocean	GISST (Parker et al. 1995)	1979–99
Sea surface salinity	ocean	NODC (Levitus et al. 1998)	variable

Table 1: Climate variables and corresponding validation data. Variables listed as “zonal mean” are latitude–height distributions of zonal averages on twelve atmospheric pressure levels between 1000 and 100 hPa. Those listed as “ocean,” “land,” or “global” are single-level fields over the respective regions. The variable “net surface heat flux” represents the sum of six quantities: incoming and outgoing shortwave radiation, incoming and outgoing longwave radiation, and latent and sensible heat fluxes. Period indicates years used to calculate observational climatologies. From (Reichler; Kim 2008) with permission.

Ocean model resolution in coupled climate models	Zonal (degree)	Meridional (degree)	Vertical (levels)
GFDL CM2.1	1.0	1.0 (telescoping to 0.3 degree near the equator)	50
UKMO-Hadcm3	1.25	1.25	20
CSIRO Mk3.5	1.875	0.93	31
MPI ECHAM5	1.0	1.0	40

Table 2: ocean model resolutions in the coupled climate models.

Contact Us
Phone: 1300 363 400
+61 3 9545 2176
Email: enquiries@csiro.au
Web: www.csiro.au

Your CSIRO

Australia is founding its future on science and innovation. Its national science agency, CSIRO, is a powerhouse of ideas, technologies and skills for building prosperity, growth, health and sustainability. It serves governments, industries, business and communities across the nation.